Environmental Pollution 218 (2016) 1108–1115

Contents lists available at ScienceDirect

Environmental Pollution

journal homepage: www.elsevier.com/locate/envpol

Fugacity gradients of hydrophobic organics across the air-water interface measured with a novel passive sampler☆

Chen-Chou Wu [a, f], Yao Yao [a, f], Lian-Jun Bao [b, *], Feng-Chang Wu [c], Charles S. Wong [d], Shu Tao [e], Eddy Y. Zeng [a, b]

[a] State Key Laboratory of Organic Geochemistry, Guangzhou Institute of Geochemistry, Chinese Academy of Sciences, Guangzhou 510640, China
[b] School of Environment, Guangzhou Key Laboratory of Environmental Exposure and Health, and Guangdong Key Laboratory of Environmental Pollution and Health, Jinan University, Guangzhou 510632, China
[c] State Key Laboratory of Environmental Criteria and Risk Assessment, Chinese Research Academy of Environmental Sciences, Beijing 100012, China
[d] Richardson College for the Environment, Department of Environmental Studies and Sciences and Department of Chemistry, University of Winnipeg, Winnipeg, Manitoba R3B 2E9, Canada
[e] Laboratory of Earth Surface Processes, College of Urban and Environmental Science, Peking University, Beijing 100871, China
[f] University of Chinese Academy of Sciences, Beijing 100049, China

ARTICLE INFO

Article history:
Received 27 April 2016
Received in revised form
17 August 2016
Accepted 24 August 2016
Available online 2 September 2016

Keywords:
Air-water interface
Passive sampler
Fugacity gradient
Hydrophobic organic contaminants
Mass transfer

ABSTRACT

Mass transfer of hydrophobic organic contaminants (HOCs) across the air-water interface is an important geochemical process controlling the fate and transport of HOCs at the regional and global scales. However, few studies have characterized concentration or fugacity profiles of HOCs near both sides of the air-water interface, which is the driving force for the inter-compartmental mass transfer of HOCs. Herein, we introduce a novel passive sampling device which is capable of measuring concentration (and therefore fugacity) gradients of HOCs across the air-water interface. Laboratory studies indicated that the escaping fugacity values of polycyclic aromatic hydrocarbons (PAHs) from water to air were negatively correlated to their volatilization half-lives. Results for field deployment were consistent between the passive sampler and an active method, i.e., a combination of grab sampling and liquid-liquid extraction. In general, the fugacity profiles of detected PAHs were indicative of an accumulation mechanism in the surface microlayer of the study regions (Haizhu Lake and Hailing Bay of Guangdong Province, China), while *p,p'*-DDD tended to volatilize from water to the atmosphere in Hailing Bay. Furthermore, the fugacity profiles of the target analytes increased towards the air-water interface, reflecting the complexity of environmental behavior of the target analytes near the air-water interface. Overall, the passive sampling device provides a novel means to better characterize the air-water diffusive transfer of HOCs, facilitating the understanding of the global cycling of HOCs.

1. Introduction

Mass transfer of hydrophobic organic compounds (HOCs) across the air-water interface is an important process governing both short-range and long-range atmospheric transport mechanisms, and bears significant implications for the global cycling of HOCs (United States Environmental Protection Agency (USEPA), 2010; Wania et al., 1998; World Health Organization (WHO), 2008). Adding to the importance of such processes is the fact that many toxic and persistent organic compounds are also hydrophobic. One of the challenges for quantifying inter-compartmental processes is to measure the concentration (and therefore fugacity) gradients of HOCs across the air-water interface. In particular, the fugacity gradients on both sides of the air-water interface that control the magnitude of air-water exchange fluxes are within a few millimeters to centimeters from the interface (Liss and Slater, 1974). Therefore, estimation of inter-compartmental transfer of HOCs across the air-water interface without robust measurements of fugacity data is likely to lead to large uncertainties (Guitart et al., 2010). To date, however, almost all measurements of fugacity gradients of HOCs were conducted with grab sampling methods and passive samplers, i.e., those collected at single points away from the

☆ This paper has been recommended for acceptance by B. Nowack.
* Corresponding author.
E-mail addresses: baolianjun@jnu.edu.cn, blj727722@163.com (L.-J. Bao).

http://dx.doi.org/10.1016/j.envpol.2016.08.064
0269-7491/

air-water interface in both the atmosphere and within the water column (Guitart et al., 2010; Khairy et al., 2014; Manodori et al., 2007; Mulder et al., 2014). In addition, inter-compartmental fluxes were measured with micrometeorological methods at two different points in the atmosphere (Sandy et al., 2012; Wong et al., 2012).

Floating a chamber across the air-water interface is a commonly accepted approach for sampling gaseous molecules of biogeochemical interest, e.g., O_2, CO_2 and CH_4 (Marino and Howarth, 1993). This method is relatively simple to adopt and measurement uncertainties are not unreasonable if executed properly (Cole et al., 2010; Galfalk et al., 2013). Alternatively, passive sampling is a simple approach in field operations, as it does not require a power supply and, unlike a flux chamber, poses no disturbance to the sample matrix (Wennrich et al., 2003; Zeng et al., 2004). However, one drawback with passive sampling methods for HOCs is the long sampling time (Friedman et al., 2012); consequently, the negative effects of photodegradation on quantitation accuracy must be considered in sampler designs (Bartkow et al., 2006; Komarova et al., 2009). Therefore, a sampler design combining the floating chamber and passive sampling approaches would be able to fulfill the objective of measuring the air-water fugacity profiles of HOCs while minimizing the effects of photodegradation. Until the present study was completed, no similar sampling devices had been found in the literature.

In this paper, we present a passive sampling device (Petition No. for Patent Cooperation Treaty: PCT/CN2015/081377) to examine two classes of HOCs, i.e., polycyclic aromatic hydrocarbons (PAHs) and *p,p'*-dichlorodiphenyltrichloroethane (*p,p'*-DDT) and its metabolites (*p,p'*-DDE and *p,p'*-DDD), the sum of which is designated as DDTs. Low-density polyethylene (LDPE) was selected as the sorbent phase. Laboratory and field studies were conducted to compare the reliability and robustness of the sampling device with an active sampling technique, i.e., a combined grab sampling and liquid-liquid extraction (LLE) approach. The relative importance of some factors, such as the concentrations of HOCs near the air-water interface, affecting these profiles and hence mass transfer was also assessed.

2. Materials and methods

2.1. Materials

Standards of 28 PAHs (Table S1) were acquired from AccuStandard (New Haven, CT, USA). Isotopically labeled PAHs (chemical purity > 98.5%, isotopic purity > 99.0%), including acenaphthene-d_{10}, phenanthrene-d_{10}, chrysene-d_{12} and perylene-d_{12} (as surrogate standards) and 2-fluorobiphenyl, *p*-terphenyl-d_{14} and dibenzo[*a,h*]anthrancene-d_{14} (as internal standards), were purchased from Dr. Ehrenstorfer GmbH (Augsburg, Germany). Standard solutions of *p,p'*-DDT, *p,p'*-DDE and *p,p'*-DDD and solid standards of PCB-67, PCB-191 (as surrogate standards) and PCB-82 (as internal standard) were purchased from AccuStandard. Six deuterated compounds, i.e., *p,p'*-DDT-d_8, *p,p'*-DDD-d_8 and *p,p'*-DDE-d_8 purchased from C/D/N Isotopes (Quebec, Canada) and anthracene-d_{10}, benzo[*a*]anthracene-d_{12} and benzo[*a*]pyrene-d_{12} purchased from Cambridge Isotope Laboratories (Andover, MA), were used as performance reference compounds (PRCs).

LDPE sheets (50-μm film thickness) were purchased from TRM Manufacturing (Corona, CA, USA). Before use, LDPE sheets were cut into 200 mm × 200 mm (for field deployment), 50 mm × 50 mm (water sampling in laboratory) and 100 mm × 100 mm slices (air sampling in laboratory), which were precleaned by dialysis in hexane twice over 48 h. The precleaned LDPE slices were immersed in water:methanol (50:50 in volume) solution spiked with anthracene-d_{10} at 30 μg L^{-1} and other PRCs (benzo[*a*]anthracene-d_{12}, benzo[*a*]pyrene-d_{12}, *p,p'*-DDT-d_8, *p,p'*-DDD-d_8 and *p,p'*-DDE-d_8) at 3 μg L^{-1} until use (at least for two weeks). Three to five pieces of loaded LDPE were processed to determine the initial PRC concentrations, and another three unloaded slices were used as field and laboratory blanks, respectively, to monitor any possible external contamination during deployment, transport and sample processing.

2.2. Sampling device design and configuration

The sampling device is comprised of an external setup and a series of sampling units connected by four stainless steel support pillars (Fig. 1). The external setup consists of three parts: (1) four vertical and two horizontal stainless steel support pillars; (2) four stainless steel porous shields and a rectangular stainless steel plate; and (3) polypropylene floats to provide buoyancy and protection for the sampling device from direct sunlight and rainfall. In addition, each sampling unit consists of an LDPE sheet wrapped by medium-flow filter papers (Whatman International, England) and stainless steel porous shields to prevent coarse particles from entering the device's interior. The consecutive sampling units are placed horizontally and separated by stainless steel spacers of different thicknesses, with symmetrically decreasing intervals from the top/bottom to the middle, i.e., 36.0, 24.0, 15.7, 12.0 and 7.4 mm. These intervals can be adjusted as needed with different-sized spacers.

2.3. Laboratory microcosm study

Laboratory testing was conducted to examine the utility of the sampling device in measuring the fugacity profiles of PAHs under controlled conditions (quiescent condition; Fig. S1). A microcosm was prepared using a 148-L stainless steel jar (with a diameter of 600 mm and a height of 600 mm) containing a 70-mm layer of water spiked with 16 non-alkylated PAH compounds in an acetone solution at 0.5 μg L^{-1} each (Table S1) and mixed by gentle agitation with a glass rod for approximately 2 min. One sampling device was placed into each jar, which was sealed and shielded from light under static conditions at 25 ± 2 °C for 10 d. Three air–water microcosms, each containing a passive device without the attachment of stainless steel shields, plates and polypropylene floats were prepared; two of them (labeled as device A and B) were spiked with PAHs and the third one was a procedural blank. For a valid measurement, it is important that transfer of PAHs into the passive sampling device does not have an impact on the mass transfer potentials of PAHs from water to air, as this would lead to profiling an artificial fugacity gradient near the air-water interface.

2.4. Field deployment

Field deployment was conducted in Hailing Bay (a semi-closure bay; Fig. S2) during September 28–October 15, 2012 and January 5–23, 2013, and in Haizhu Lake (a man-made wetland; Fig. S2) during September 29–October 16, 2012. These sites are located near heavy boat and automobile traffic, respectively, and PAHs may be discharged from engine exhaust. Previous studies also detected abundant DDTs in the water of Hailing Bay, with *p,p'*-DDD as the predominant constituent (Yu et al., 2011a, 2011b). At each site, one sampling device consisting of consecutive sampling units was floated on the water surface and anchored with concrete bricks (Fig. S3a), collecting freely dissolved HOCs on both sides of (close to) the air-water interface. In addition, several individual passive sampling units used for bulk matrix measurements were fixed at various distances from both sides of the air-water interface, i.e., 60,

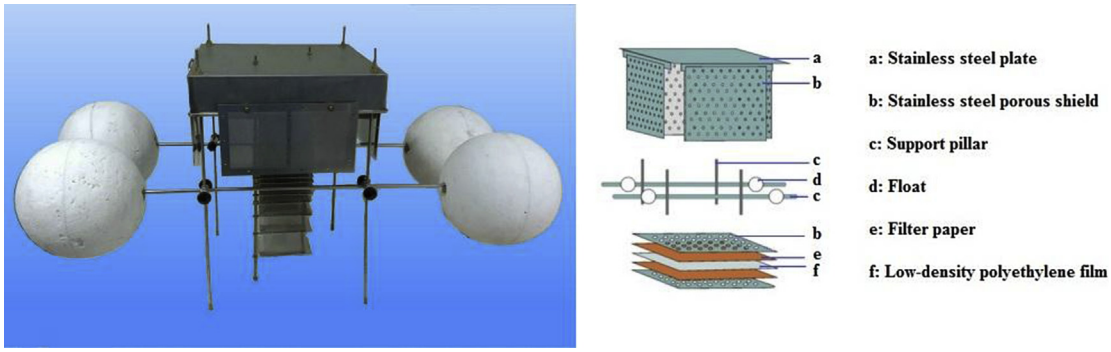

Fig. 1. Configuration of the passive sampling device.

300 and 2000 mm above and 60, 1000, 2000 and 3000 mm below the air-water interface in Hailing Bay, and 60, 300 and 5000 mm above and 60 mm below the air-water interface in Haizhu Lake. The air-side sampling units were shaded from sunlight with a stainless steel plate, separated by stainless steel spacers and placed horizontally (Fig. S3b). One to two passive samplers, as replicates, was lost in each sampling period. Upon completion of deployment, the sampling devices and sampling units were disassembled, and the LDPE slices were retrieved and transported under ice to the laboratory, where they were stored at −20 °C until analysis.

Water surface microlayer samples were collected with a glass plate (~50 cm × 60 cm) dipped vertically through the water surface and withdrawn at a constant speed of approximately 15 cm s^{-1} (Harvey and Burzell, 1972), removed from both sides of the plate with a silicone rubber squeegee blade, and stored in a glass vial. Five liters of each sample were collected in Hailing Bay, while 0.5 L was collected in Haizhu Lake. Surface water samples from ~0.5 m beneath the air-water interface were collected with a stainless steel submersible pump into 10-L brown glass bottles. All water samples ($n = 8$) were stored at 4 °C and processed within 24 h.

2.5. Sample extraction

Loaded LDPE slices were rinsed with Milli-Q water (18 MΩ-cm, Millipore) water and wiped with filter paper to remove residual water on the slices. They were cut to small pieces (~20 mm × 30 mm), wrapped with filter paper, spiked with the surrogate standards, and extracted in hexane (soaking) twice over 24 h. Each extract was concentrated to 1 mL with a Zymark TurboVap 500 (Hopkinton, MA), and the final extract was spiked with the internal standards before instrumental analysis.

Water samples were filtered with glass fiber filtration membranes (GF/F; 0.7 μm nominal pore size; Whatman International), and the filtrates were liquid–liquid extracted three times with 80, 60 and 40 mL of dichloromethane after addition of the surrogate standards. Each combined extract was purified with a glass chromatography column containing 3% deactivated neutral silica gel (120 mm) and neutral alumina (60 mm) from top to bottom. Finally, internal standards were added to the final extract after it was concentrated to 100 μL under a gentle stream of nitrogen. All extracts were analyzed with GC-MS. Detailed instrumental procedures and quality assurance and quality control results are provided in Text S1.

2.6. Data analysis

The gaseous concentration in air (C_a; ng m^{-3}) or freely dissolved concentration (C_w; ng L^{-1}) in water of a target compound was derived from the PE-normalized concentration ($C_{pe\text{-}a}$ or $C_{pe\text{-}w}$) divided by the sampling rate ($R_{s\text{-}a}$; m^3 d^{-1} for air or $R_{s\text{-}w}$; L d^{-1} for water) of the target compound and the equilibrium partition coefficient of PE–air ($K_{pe\text{-}a}$; L kg^{-1}) or PE–water ($K_{pe\text{-}w}$; L kg^{-1}) (Lohmann et al., 2012), i.e.,

$$C_a = \frac{C_{pe-a}}{K_{pe-a} \times \left[1 - \exp\left(-\frac{R_{s-a}t}{K_{pe-a}M_{pe}}\right)\right]} \quad (1)$$

$$C_w = \frac{C_{pe-w}}{K_{pe-w} \times \left[1 - \exp\left(-\frac{R_{s-w}t}{K_{pe-w}M_{pe}}\right)\right]} \quad (2)$$

The sampling rates of target compounds can be derived from the sampling rates of PRCs ($R_{s\text{-}PRC}$) by adjusting R_s for the difference in the partition coefficients. The sampling rates ($R_{s\text{-}PRC}$) of PRCs can be estimated by the fractions of PRCs remaining in the PE sampler (f_{PRC}). The values of $K_{pe\text{-}a}$ or $K_{pe\text{-}w}$ were acquired from previous studies (Bao et al., 2012; Khairy et al., 2014; Reitsma et al., 2013) and corrected for temperature by the van't Hoff equation and for salinity by the Setschenow constant (Schwarzenbach et al., 2003). The Setschenow constant (K_{Si}; L mol^{-1}) used was 0.3 for PAHs (Schwarzenbach et al., 2003) and 0.35 for DDTs (Lohmann, 2012). M_{pe} is the mass of PE (kg). More details on calculation of sampling rates for PRCs and target compounds and corrections of $K_{pe\text{-}a}$ and $K_{pe\text{-}w}$ are given in Texts S2 and S3. The parameters used to calculate C_a and C_w of the target compounds are listed in Tables S1 and S2.

The fugacity of an analyte in air (f_a; Pa) and water (f_w; Pa), as well as the fugacity fraction (f), can be obtained by (Liss and Slater, 1974; Mackay and Paterson, 1991; Wong et al., 2012):

$$f_a = C_a \times R \times T_A / M \quad (3)$$

$$f_w = C_w \times H / M \quad (4)$$

$$f = f_a(y) / f_a(y) + f_w(y') \quad (5)$$

where R is the ideal gas constant (8.314 Pa m^3 K^{-1} mol^{-1}); T_A is the air temperature (K); M is the molecular weight of the target analyte (g mol^{-1}); H is the Henry's Law constant (Pa m^3 mol^{-1}); $f_a(y)$ represents the fugacity in air at distance y from the air-water interface and $f_w(y')$ represents the fugacity in water at distance y' from the air-water interface. Surface microlayer may have a higher fugacity capacity constant than bulk water (Southwood et al., 1999); however, freely dissolved concentrations rather than bulk concentrations of target analytes were derived by the LDPE slice sampler. As a result, equation (4) is suitable for estimating fugacity in surface microlayer. A value of f of 0.5, <0.5 or >0.5 indicates, respectively,

equilibrium between air and water, net volatilization from water to air, or deposition from air to water for a target analyte (Wong et al., 2012).

To identify the impacts of the variability of the related parameters on the fugacity, uncertainty ranges in the fugacities and fugacity fractions of the target analytes were estimated using Monte Carlo simulation, which was performed with Crystal Ball® software (Version 2000.2, Decisioneering, Denver, CO, USA). Sensitive analysis and propagation of error analysis were performed with Monte Carlo simulation and Microsoft Excel 2010, respectively. Detailed values and distributions for all variables (such as $K_{pe\text{-}a}$, $K_{pe\text{-}w}$, H and f_{PRC}) are provided in Tables S1 and S2.

3. Results and discussion

3.1. Sampler design considerations and effects of turbulence

The field results showed that the average loss fractions of benzo[*a*]pyrene-d_{12}, used to assess the effects of photodegradation, ranged from 10% to 26% (Table S3). The dissipation rates of benzo[*a*]pyrene-d_{12} (air: 0.016 ± 0.011 d^{-1}; water: 0.015 ± 0.010 d^{-1}) in the field deployment were not significantly different from those in the laboratory microcosms (air: 0.013 ± 0.008 d^{-1}; water: 0.014 ± 0.012 d^{-1}, $p > 0.05$, paired-sample *t*-test), demonstrating no significant photodegradation during field deployment. This indicated that the sampler design was effective in minimizing photodegradation of sorbed analytes in the sorbent phase, as the sorbents were shielded with a rectangular stainless steel plate and wrapped with filter paper.

A previous study also used dibenz[*a,h*]anthracene-d_{14} for assessment of photodegradation effects in semipermeable membrane devices (SPMDs) deployed in the ocean for 33 d (Komarova et al., 2009). No detectable loss of dibenz[*a,h*]anthracene-d_{14} was found in samplers housed in typical SPMD cages covered with mesh, whereas the loss of dibenz[*a,h*]anthracene-d_{14} reached 86% for samplers without any protection and was 27% for samplers with porous cages as outer shields (Komarova et al., 2009). Apparently, shielding from light is the key to minimizing the effects of photodegradation in passive sampler design.

The field results showed that the fugacity values of PAHs and *p,p'*-DDD derived by two passive sampling methods at the same sampling heights (60 mm above the air-water interface) at two sampling sites were not significantly different (Table 1; $p > 0.05$, paired-sample *t*-test). This indicated that the design of consecutive sampling units within the passive sampler design was able to minimize the effects of artificially introduced turbulence on the sampling microenvironment, although the passive sampling device bounced around with waves in field deployment.

3.2. Laboratory microcosm results

After 240 h of mimicked volatilization from water to air in the microcosm, the amount of low-ring PAHs, such as acenaphthylene, acenaphthene and fluorine, that accumulated in the passive sampling device accounted for 18–30% of their initially spiked amounts (Table S5). Furthermore, the sampling time (~240 h) was far longer than the predicted half-lives (4.4–7.4 h; Table S6), suggesting that the fugacity gradient of PAHs would only be slightly influenced, at most, by the passive sampling device.

The fugacity profiles of target PAHs in water showed increasing trends toward the air-water interface (Figs. 2 and S4). This was probably because surface viscoelastic effects and/or surface tension significantly reduced the gas transfer rate (Frew, 1997), which would result in chemical accumulation near the air-water interface. Such a finding is consistent with the fact that changes in concentration profiles of gases mainly occur within a few millimeters of the air-water interface (Liss and Slater, 1974). On the air side, the fugacity profiles of acenaphthylene, acenaphthene, fluorene, phenanthrene, anthracene, fluoranthene and pyrene are presented almost as a straight line, indicating a near-equilibrium state for these compounds (Fig. 2a–g). However, of the high-ring PAHs, only benzo[*a*]anthrancene was detected near the air-water interface (Fig. 2h–n). These results were in agreement with the fact that three- and some four-ring PAHs have shorter volatilization half-lives than higher-ring PAHs (Table S6).

Low-ring PAHs may volatilize from water, as indicated by the short volatilization half-lives of naphthalene (0.4–6.2 h) and anthracene (12–17 h) (Table S6) (Southworth, 1979). High-ring PAHs, however, have volatilization half-lives ranging from 130 to 5300 h (Table S6). The sampling time of laboratory microcosm in the present study (~240 h) was longer than the predicted half-lives of low-ring PAHs (<100 h; Table S6). The nearly equal fugacity profiles of low-ring PAHs between air and water were indicative of a near-equilibrium state (Fig. 2a–g). On the other hand, the sampling time was much shorter than the predicted half-lives of high-ring PAHs (130–5300 h; Table S6), resulting in net vaporization for these compounds consistent with observed fugacity differences between air and water (Fig. 2h–n). Overall, these results demonstrated that the sampling device was able to measure air-water concentration profiles of PAHs under controlled laboratory conditions.

3.3. Field validation

During the sampling period of September–October 2012, the concentrations of PAHs at both sites obtained by the active sampling method (grab sampling with glass plate) were greater in surface microlayer samples than in seawater (130–830 ng L^{-1} versus 10–60 ng L^{-1}; Table 2). For DDTs, only *p,p'*-DDD was detected in Hailing Bay water samples, and its concentrations were greater in seawater (0.6–0.9 ng L^{-1}) than in the surface microlayer (not detected) (Table 2). In addition, three- and four-ring PAHs were the main PAH components in all water samples, particularly phenanthrene (12–32%), fluoranthene (17–39%) and pyrene (9–27%) (Table 2).

The fugacity profiles of phenanthrene, fluoranthene, pyrene and methyl-phenanthrenes in the ambient air of Haizhu Lake obtained by several individual passive sampling units showed decreasing trends from 5 m toward the air-water interface (Figs. S5a–S5b and S5e–S5f). In addition, there was net deposition of phenanthrene, fluoranthene, pyrene and alkyl-phenanthrenes from air to water in Hailing Bay (Figs. S6a–S6e and S6g and Table S7), but *p,p'*-DDD tended to volatilize from water to air (Fig. S6h and Table S7).

The fugacity profiles of PAHs and DDTs near both sides of the air-water interface in Haizhu Lake and Hailing Bay were also obtained by the passive sampling device consisting of consecutive sampling units (Figs. 3 and 4 and S7). Meanwhile, the fugacities of 2-methylphenanthrene, 4+9-methylphenanthrene, 2,6-dimethylphenanthrene, fluoranthene, 3-methylphenanthrene and *p,p'*-DDD (Figs. 4b–e, 4g-4h and S7c) increased towards the air-water interface ($p < 0.05$, one-sample *t*-test). A similar phenomenon was also observed in the visualization of oxygen air-water exchange using novel fluorescent dyes, with a sharp decrease of luminescence intensity (due to the absorption of fluorescent dyes by dissolved oxygen) observed near the air-water interface (Falkenroth et al., 2006).

The sensitivity analysis (Fig. S8) showed that the PE-air equilibrium partition coefficient of a target compound ($K_{pe\text{-}a}$) was the major contributor to the uncertainty of fugacity in field deployments, with a sensitivity contribution in the range of 67–88%.

Table 1
Fugacities of polycyclic aromatic hydrocarbons (PAHs; $\times 10^{-9}$ Pa) and *p,p'*-DDD ($\times 10^{-9}$ Pa) derived by two passive sampling methods at same sampling heights in Haizhu Lake and Hailing Bay of Guangdong Province, China.

	Haizhu Lake (September 29–October 16, 2012)		Hailing Bay (September 28–October 15, 2012)	
	Consecutive sampling units	Passive sampling unit	Consecutive sampling units	Passive sampling unit
air side (60 mm above the air-water interface)				
phenanthrene	18.9	18.4	5.5	3.7
2-methylphenanthrene	0.7	0.6	0.8	0.6
4+9-methylphenanthrene	0.8	0.9	0.7	0.6
2,6-dimethylphenanthrene	0.1	0.1	0.2	0.1
fluoranthene	1.3	1.0	0.2	0.2
pyrene	0.9	0.6	0.8	0.7
3-methylphenanthrene	0.5	0.5	0.7	0.5
1,7-dimethylphenanthrene	0.2	0.2	–	–
p,p'-DDD	–	–	0.7	0.1
water side (60 mm below the air-water interface)				
phenanthrene	7.6	9.7	4	0.9
2-methylphenanthrene	0.4	1.1	0.7	0.2
4+9-methylphenanthrene	0.3	1.5	0.5	0.3
2,6-dimethylphenanthrene	0.1	0.2	0.1	0.05
fluoranthene	0.8	1.4	0.2	0.1
pyrene	1.1	2.1	0.1	0.2
3-methylphenanthrene	0.5	1.1	0.1	0.2
1,7-dimethylphenanthrene	0.3	0.8	–	–
p,p'-DDD	–	–	0.06	0.06

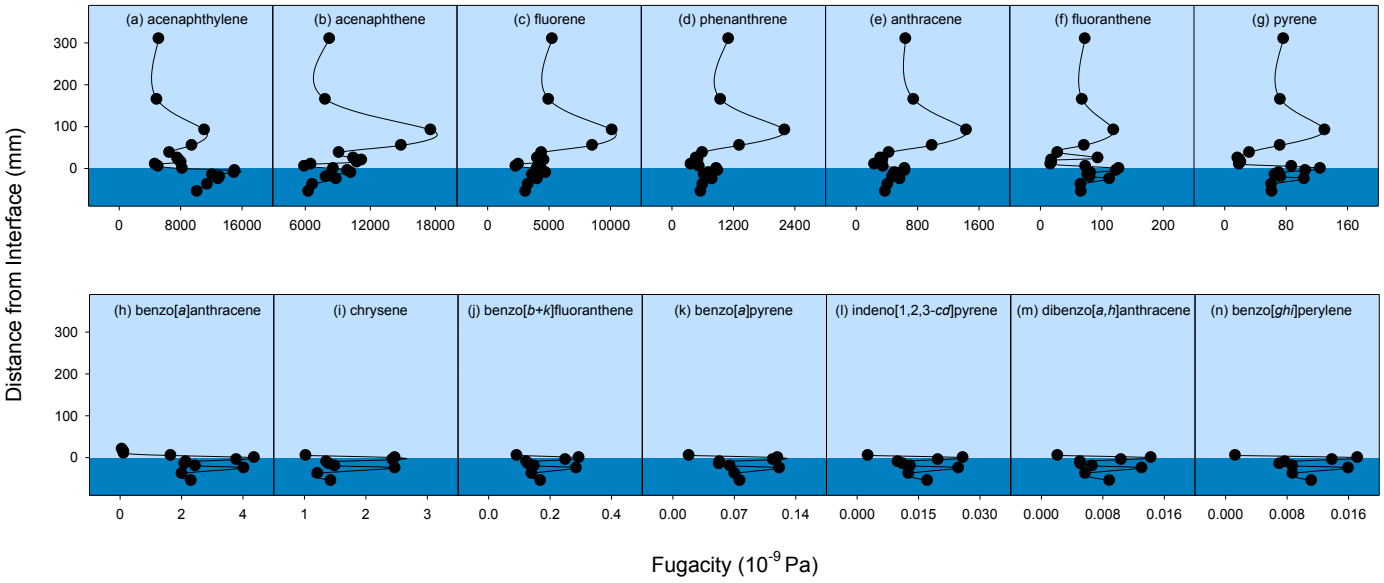

Fig. 2. Vertical fugacity profiles of PAHs obtained with the passive sampling device consisting of consecutive sampling units (device A) in laboratory air-water microcosms. The sampling time was 10 days, and two parallel systems were set up at 25 ± 2 °C. The blue and deep blue portions represent air and water, respectively. The concentrations of higher weigh molecular PAHs (benzo[*a*]anthrancene, chrysene, benzo[*b*+*k*]fluoranthene, benzo[*a*]pyrene, indeno[*1,2,3-cd*]pyrene, dibenzo[*a, h*]anthrancene and benzo[*ghi*]perylene) in air-side were below the reporting limits. (For interpretation of the references to colour in this figure legend, the reader is referred to the web version of this article.)

Furthermore, the PE-water equilibrium partition coefficient ($K_{pe\text{-}w}$) and Henry's Law constant (H) accounted for 66–70% and 36–55% of the fugacity uncertainty, respectively. In contrast, the retained fractions of PRCs were insensitive to the fugacity uncertainty. In addition, the overall propagated errors (Text S1) associated with fugacities ranged from 50% (phenanthrene) to 64% (2,6-dimethylphenanthrene) in air and 71–131% in water with the average values at 57% and 85%, respectively. Most propagated errors of PAHs fugacities were attributed to the PE-equilibrium partition coefficients, with the average contributions from $K_{pe\text{-}a}$ and $K_{pe\text{-}w}$ at 80% and 50%, respectively. These findings highlight the need to accurately determine the PE-air or PE-water equilibrium partition coefficient of a target compound.

As a passive sampler only accumulates dissolved or gaseous PAHs in water or air, respectively, the equilibrium concentrations of PAHs thus accumulated ($C_{pe\text{-}w,eq}$ and $C_{pe\text{-}a,eq}$) would be proportional to the activities of PAHs at a constant temperature. To reduce the uncertainty of fugacity gradients, the equilibrium concentrations ($C_{pe\text{-}w,eq}$ and $C_{pe\text{-}a,eq}$) of PAHs in the sampler, which were estimated only by the PAH concentrations in PE and the lost fractions of PRCs (Text S4), were used to corroborate the fugacity gradients near the air-water interface. As expected, equilibrium concentration profiles of PAHs in the sampler (Fig. S10) were consistent with the fugacity profiles (Fig. 3).

In summary, fugacity profiles obtained by the present passive sampling device showed variable trends with different target analytes. The fugacity profiles of detected PAHs were indicative of accumulation near both sides of the air-water interface, whilst *p,p'*-

Table 2
Concentrations of dissolved polycyclic aromatic hydrocarbons (PAHs; ng L^{-1}) and dichlorodiphenyltrichloroethane and its metabolites (ng L^{-1}) in the surface water (SW) and surface microlayer (SML) water collected in Haizhu Lake and Hailing Bay of Guangdong Province, China.

	Haizhu Lake				Hailing Bay			
Sampling time	September 29, 2012		October 16, 2012		September 28, 2012		October 15, 2012	
Temperature and Pressure	20–31 °C; 0 psu				23–29 °C; 35 psu			
	SW	SML	SW	SML	SW	SML	SW	SML
p,p'-DDT	ND[a]	ND	ND	ND	ND	ND	ND	ND
p,p'-DDD	ND	ND	ND	ND	0.9	ND	0.6	ND
p,p'-DDE	ND	ND	ND	ND	ND	ND	ND	ND
phenanthrene	6.5	36	7.5	51	2.0	286	2.2	89
3-methylphenanthrene	3.4	7.4	2.4	17	0.8	51	1.0	34
2-methylphenanthrene	3.7	5.7	3.8	23	1.3	64	1.1	40
4+9-methylphenanthrene	3.3	10	1.8	14	0.6	38	0.8	35
2,6-dimethylphenanthrene	9.8	6.0	1.0	6.0	1.0	32	0.9	10
1,7-dimethylphenanthrene	6.0	3.0	1.0	4.0	1.0	32	1.6	21
fluoranthene	17	22	7.2	117	2.8	200	3.6	48
pyrene	7.5	35	4.9	74	1.3	126	1.3	26
$\sum_8$PAH	57	125	30	306	11	829	13	304

[a] ND: not detected.

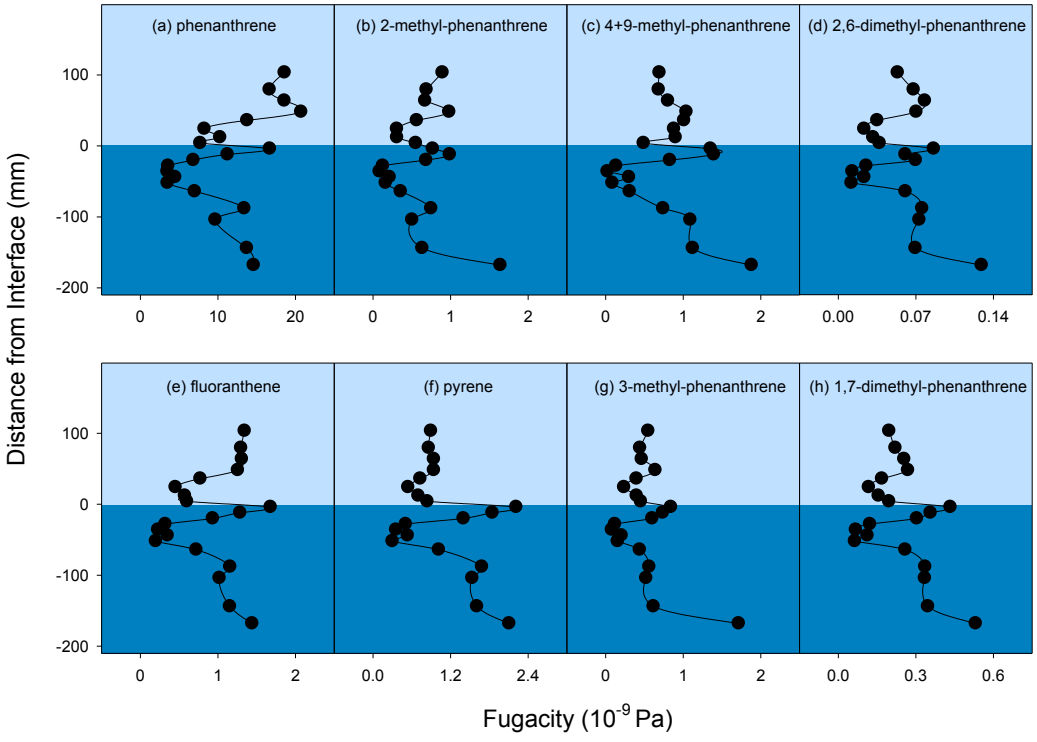

Fig. 3. Vertical fugacity profiles of PAHs obtained by the passive sampling device consisting of consecutive sampling units in Haizhu Lake of Guangzhou, China, during September 29–October 16, 2012. The blue and deep blue portions represent air and water, respectively. (For interpretation of the references to colour in this figure legend, the reader is referred to the web version of this article.)

DDD in Hailing Bay tended to escape from water to the atmosphere. In addition, the trends for fugacity profiles obtained by the active sampling (grab sampling with glass plate) and passive sampling methods (passive sampling devices consisting of consecutive sampling units and individual passive sampling units) were consistent.

3.4. Significance of concentration gradients of HOCs near the air-water interface

It is obvious that air-water transfer of HOCs is largely dictated by the interface between the gaseous and liquid phases. Within the air-water interface, the surface microlayer is a thin boundary layer containing abundant organic matter. It is the link between the hydrosphere and the atmosphere (Cunliffe et al., 2013); thereby it plays a significant role in the inter-compartmental transfer of HOCs and must be adequately considered. For example, a surfactant film, an enriched layer of organic surfactants in the surface microlayer, can retard gas exchange (McKenna and McGillis, 2004). Calleja et al. (2009) reported that high levels of surface organic matter (TOC > 90 mol C L^{-1}; CO_2 fluxes: -3.1 ± 5.1 mmol C m^2 d^{-1}) led to lower air-water CO_2 fluxes than those with low organic matter content (TOC < 90 mol C L^{-1}; CO_2 fluxes: -22 ± 27 mmol C m^2 d^{-1}). The mass transfer velocity related to wind speed was also

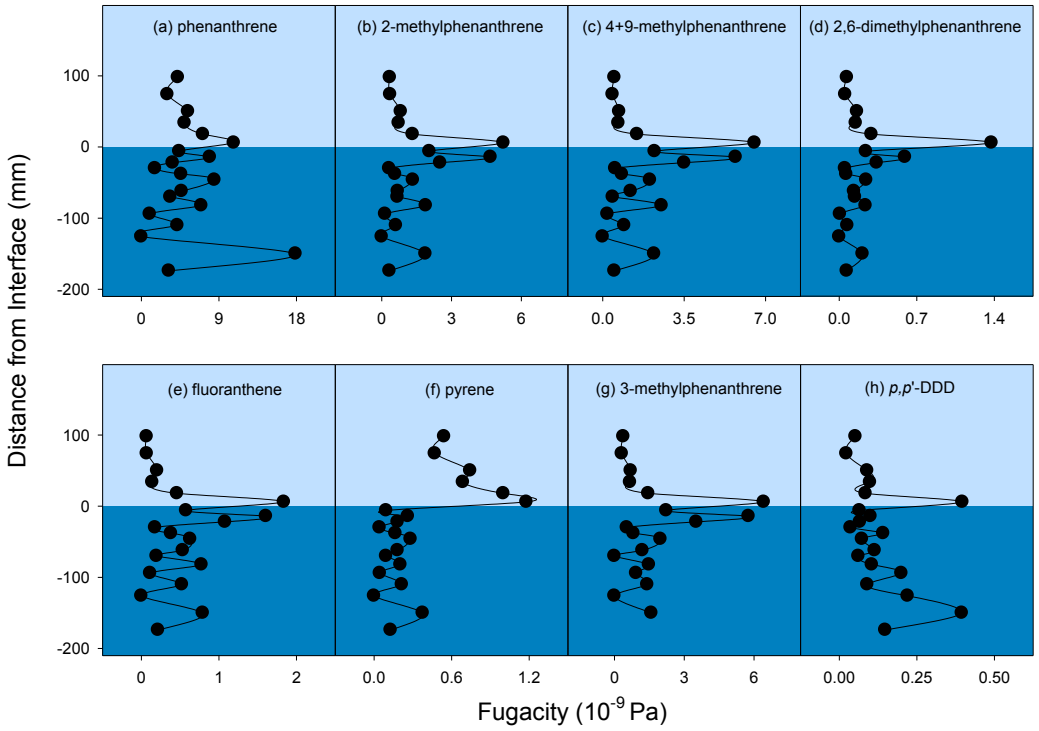

Fig. 4. Vertical fugacity profiles of PAHs and *p,p'*-DDD obtained by the passive sampling device consisting of consecutive sampling units in Hailing Bay of Guangdong Province, China, during September 28–October 15, 2012. The blue and deep blue portions represent air and water, respectively. (For interpretation of the references to colour in this figure legend, the reader is referred to the web version of this article.)

overestimated in the presence of surface films (Frew et al., 2004). Moreover, HOCs can interact with organic surfactants because of their hydrophobicity (Acharid et al., 2006; Sadiki et al., 2003), which may lead to suppression (sorption to organic matter) or enhancement (surfactants-micellar solubilization) of air-water exchange of HOCs. Such resistance or assistance to mass transfer across the air-water interface can be assessed by concentration gradients on either side of the air-water interface (Cunliffe et al., 2013). Characterization of surface microlayer, such as its thickness and fugacity or concentration gradients near the air-water interface, is thus important for understanding air-water exchange of HOCs. However, both the thickness of the surface microlayer and the fugacity (or concentration) gradient of HOCs are often difficult to measure, particularly with conventional techniques (Liss and Slater, 1974; Rowe and Perlinger, 2012). There is ample evidence that the surface microlayer can accumulate larger amounts of HOCs than bulk water (Garcia-Flor et al., 2005; McMurdo et al., 2008; Wurl and Obbard, 2005), as we observed for PAHs (Table 2). Yet it is not entirely clear how the microlayer affected fluxes of HOCs across the air-water interface in the present study, which focused on methods to characterize the fugacity profiles near the interface. Because of physical restraints of the sampler configurations and strong wave turbulence, the present passive sampling device was unable to measure analyte concentrations within the surface microlayer. As a result, assessment of fluxes is beyond the scope of the current study.

The present study demonstrated that sampling of single points in air and overlying water is unable to obtain fugacity gradients of HOCs across the air-water interface, because chemical fugacity near the air-water interface may differ substantially from that within bulk matrices. For example, bulk matrix measurements at single points suggested that fluoranthene and some alkyl-phenanthrenes tended to deposit from air to water in Hailing Bay (Fig. S6b–S6e). However, the fugacity profiles of these compounds obtained by the passive sampling device with relatively high resolution were indicative of a near-equilibrium state (Figs. 4b–4e). Furthermore, the trends of fugacity profiles increased as towards the air-water interface (Figs. 3b and 3d–3h and Figs. 4b–4e and 4g), which would also add to the uncertainties of air-water diffusional fluxes besides the intrinsic errors from the use of physiochemical parameters such as Henry's Law constants, partition coefficients and overall mass transfer coefficients (Gioia et al., 2010; Wong et al., 2012). An extreme example is the variability in the fugacity fractions of phenanthrene and fluoranthene, which varied from $f = 0.80–0.86$ indicating deposition, to $f = 0.21–0.33$ indicating volatilization, depending on where the measurements were taken (Table S8). This finding was further corroborated by the air-water exchange ratios of PAHs estimated from the equilibrium concentrations in the sampler (Fig. S11). Therefore, high-resolution measurement of the concentrations of HOCs near the air-water interface is essential for any attempt to better understand the transport and fate of HOCs at both the local and global scales.

4. Conclusions

A novel passive sampler with LDPE as sorbent phase was introduced and validated to be capable of measuring the fugacity profiles of HOCs across the air-water interface. In the laboratory microcosm study, the escaping fugacity values of PAHs from water to air were negatively correlated to their volatilization half-lives. Field deployment results demonstrated that the detected PAHs were likely to accumulate near both sides of the air-water interface, whilst *p,p'*-DDD in Hailing Bay tended to escape from water to the atmosphere. In addition, the variability in the fugacity fractions of phenanthrene and fluoranthene depended on the where the measurements were taken, suggesting that it is crucial to take a

high spatial resolution measurement within the air-water interface to understand the transport and fate of HOCs.

Acknowledgments

The present study was financially supported by the National Natural Science Foundation of China (Nos. 41390240 and 41403087), the Ministry of Science and Technology of China (No. 2012ZX07503-003-002), the Natural Sciences and Engineering Research Council of Canada, and the Canada Research Chairs Program. The authors are grateful to Wei-Hao Feng, Yan-Li Wei, Ru-Lang Shen, and Zai-Cheng He for sample collection. This is contribution No. IS-2291 from GIGCAS.

Appendix A. Supplementary data

Supplementary data related to this article can be found at http://dx.doi.org/10.1016/j.envpol.2016.08.064.

References

Acharid, A., Quentel, F., Elleouet, C., Olier, R., Privat, M., 2006. Coadsorption of carbofuran and lead at the air/water interface. Possible occurrence of non-volatile pollutant cotransfer to the atmosphere. Chemosphere 62, 989–997.

Bao, L.-J., Xu, S.-P., Liang, Y., Zeng, E.Y., 2012. Development of a low-density polyethylene-containing passive sampler for measuring dissolved hydrophobic organic compounds in open waters. Environ. Toxicol. Chem. 31, 1012–1018.

Bartkow, M.E., Kennedy, K.E., Huckins, J.N., Holling, N., Komarova, T., Mueller, J.F., 2006. Photodegradation of polyaromatic hydrocarbons in passive air samplers: field testing different deployment chambers. Environ. Pollut. 144, 371–376.

Calleja, M.L., Duarte, C.M., Prairie, Y.T., Agusti, S., Herndl, G.J., 2009. Evidence for surface organic matter modulation of air-sea CO_2 gas exchange. Biogeosciences 6, 1105–1114.

Cole, J.J., Bade, D.L., Bastviken, D., Pace, M.L., Van de Bogert, M., 2010. Multiple approaches to estimating air-water gas exchange in small lakes. Limnol. Oceanogr. Methods 8, 285–293.

Cunliffe, M., Engel, A., Frka, S., Gasparovic, B., Guitart, C., Murrell, J.C., Salter, M., Stolle, C., Upstill-Goddard, R., Wurl, O., 2013. Sea surface microlayers: a unified physicochemical and biological perspective of the air-ocean interface. Prog. Oceanogr. 109, 104–116.

Falkenroth, A., Herzog, A., Jähne, B., 2006. Visualization of air-water gas exchange using novel fluorescent dyes. The 12th International Symposium on Flow Visualization, Göttingen, Germany.

Frew, N.M., 1997. Chapter 5: the role of organic films in air-sea gas exchange. In: Liss, P.S., Duce, R.A. (Eds.), The Sea Surface and Global Change. Cambridge University Press, Cambridge, U.K, pp. 121–172.

Frew, N.M., Bock, E.J., Schimpf, U., Hara, T., Haussecker, H., Edson, J.B., McGillis, W.R., Nelson, R.K., McKenna, S.P., Uz, B.M., Jahne, B., 2004. Air-sea gas transfer: its dependence on wind stress, small-scale roughness, and surface films. J. Geophys. Res. Oceans 109, C08S17.

Friedman, C.L., Cantwell, M.G., Lohmann, R., 2012. Passive sampling provides evidence for Newark Bay as a source of polychlorinated dibenzo-*p*-dioxins and furans to the New York/New Jersey, USA, atmosphere. Environ. Toxicol. Chem. 31, 253–261.

Galfalk, M., Bastviken, D., Fredriksson, S.T., Arneborg, L., 2013. Determination of the piston velocity for water-air interfaces using flux chambers, acoustic Doppler velocimetry, and IR imaging of the water surface. J. Geophys. Res. Biogeosci. 118, 770–782.

Garcia-Flor, N., Guitart, C., Abalos, M., Dachs, J., Bayona, J.M., Albaiges, J., 2005. Enrichment of organochlorine contaminants in the sea surface microlayer: an organic carbon-driven process. Mar. Chem. 96, 331–345.

Gioia, R., Jones, K.C., Lohmann, R., Nizzetto, L., Dachs, J., 2010. Field-derived Henry's law constants for polychlorinated biphenyls in oceanic waters. J. Geophys. Res. Oceans 115, C05024.

Guitart, C., Garcia-Flor, N., Miquel, J.C., Fowler, S.W., Albaiges, J., 2010. Effect of the accumulation of polycyclic aromatic hydrocarbons in the sea surface microlayer on their coastal air-sea exchanges. J. Mar. Syst. 79, 210–217.

Harvey, G.W., Burzell, L.A., 1972. Simple microlayer method for small samples. Limnol. Oceanogr. 17, 156–157.

Khairy, M., Muir, D., Teixeira, C., Lohmann, R., 2014. Spatial trends, sources, and air-water exchange of organochlorine pesticides in the Great Lakes basin using low density polyethylene passive samplers. Environ. Sci. Technol. 48, 9315–9324.

Komarova, T.V., Bartkow, M.E., Rutishauser, S., Carter, S., Mueller, J.F., 2009. Evaluation and in situ assessment of photodegradation of polyaromatic hydrocarbons in semipermeable membrane devices deployed in ocean water. Environ. Pollut. 157, 731–736.

Liss, P.S., Slater, P.G., 1974. Flux of gases across the air-sea interface. Nature 247, 181–184.

Lohmann, R., 2012. Critical review of low-density polyethylene's partitioning and diffusion coefficients for trace organic contaminants and implications for its use as a passive sampler. Environ. Sci. Technol. 46, 606–618.

Lohmann, R., Booij, K., Smedes, F., Vrana, B., 2012. Use of passive sampling devices for monitoring and compliance checking of POP concentrations in water. Environ. Sci. Pollut. Res. 19, 1885–1895.

Mackay, D., Paterson, S., 1991. Evaluating the multimedia fate of organic chemicals: a level III fugacity model. Environ. Sci. Technol. 25, 427–436.

Manodori, L., Gambaro, A., Moret, I., Capodaglio, G., Cescon, P., 2007. Air-sea gaseous exchange of PCB at the Venice lagoon (Italy). Mar. Pollut. Bull. 54, 1634–1644.

Marino, R., Howarth, R.W., 1993. Atmospheric oxygen-exchange in the hudson river-dome measurements and comparison with other natural-waters. Estuaries 16, 433–445.

McKenna, S.P., McGillis, W.R., 2004. The role of free-surface turbulence and surfactants in air-water gas transfer. Int. J. Heat Mass Transf. 47, 539–553.

McMurdo, C.J., Ellis, D.A., Webster, E., Butler, J., Christensen, R.D., Reid, L.K., 2008. Aerosol enrichment of the surfactant PFO and mediation of the water-air transport of gaseous PFOA. Environ. Sci. Technol. 42, 3969–3974.

Mulder, M.D., Heil, A., Kukucka, P., Klanova, J., Kuta, J., Prokes, R., Sprovieri, F., Lammel, G., 2014. Air-sea exchange and gas-particle partitioning of polycyclic aromatic hydrocarbons in the Mediterranean. Atmos. Chem. Phys. 14, 8905–8915.

Reitsma, P.J., Adelman, D., Lohmann, R., 2013. Challenges of using polyethylene passive samplers to determine dissolved concentrations of parent and alkylated PAHs under cold and saline conditions. Environ. Sci. Technol. 47, 10429–10437.

Rowe, M.D., Perlinger, J.A., 2012. Micrometeorological measurement of hexachlorobenzene and polychlorinated biphenyl compound air-water gas exchange in Lake Superior and comparison to model predictions. Atmos. Chem. Phys. 12, 4607–4617.

Sadiki, M., Quentel, F., Elleouet, C., Huruguen, J.P., Jestin, J., Andrieux, D., Olier, R., Privat, M., 2003. Coadsorption at the air/water interface likely explains some pollutants transfer to the atmosphere: benzene and lead case. Atmos. Environ. 37, 3551–3559.

Sandy, A.L., Guo, J., Miskewitz, R.J., McGillis, W.R., Rodenburg, L.A., 2012. Fluxes of polychlorinated biphenyls volatilizing from the Hudson River, New York measured using micrometeorological approaches. Environ. Sci. Technol. 46, 885–891.

Schwarzenbach, R.P., Gschwend, P.M., Imboden, D.M., 2003. Environmental Organic Chemistry, second ed. John Wiley & Sons, New Jersey, NY, United States.

Southwood, J.M., Muir, D.C.G., Mackay, D., 1999. Modelling agrochemical dissipation in surface microlayers following aerial deposition. Chemosphere 38, 121–141.

Southworth, G.R., 1979. The role of volatilization in removing polycyclic aromatic hydrocarbons from aquatic environments. Bull. Environ. Contam. Toxicol. 21, 507–514.

United States Environmental Protection Agency (USEPA), 2010. International Transport of Air Pollution. www.epa.gov/airtrends/2010/report/intltransport.pdf (accessed 20.04.16.).

Wania, F., Axelman, J., Broman, D., 1998. A review of processes involved in the exchange of persistent organic pollutants across the air-sea interface. Environ. Pollut. 102, 3–23.

Wennrich, L., Vrana, B., Popp, P., Lorenz, W., 2003. Development of an integrative passive sampler for the monitoring of organic water pollutants. J. Environ. Monit. 5, 813–822.

Wong, F., Jantunen, L., Papakyriakou, T., Staebler, R., Stern, G., Bidleman, T., 2012. Comparison of micrometeorological and two-film estimates of air-water gas exchange for alpha-hexachlorocyclohexane in the Canadian archipelago. Environ. Sci. Pollut. Res. 19, 1908–1914.

World Health Organization (WHO), 2008. Persistent Organic Pollutants (POPs). www.who.int/ceh/capacity/POPs.pdf (accessed 20.04.16.).

Wurl, O., Obbard, J.P., 2005. Chlorinated pesticides and PCBs in the sea-surface microlayer and seawater samples of Singapore. Mar. Pollut. Bull. 50, 1233–1243.

Yu, H.-Y., Guo, Y., Bao, L.-J., Qiu, Y.-W., Zeng, E.Y., 2011a. Persistent halogenated compounds in two typical marine aquaculture zones of South China. Mar. Pollut. Bull. 63, 572–577.

Yu, H.-Y., Shen, R.-L., Liang, Y., Cheng, H., Zeng, E.Y., 2011b. Inputs of antifouling paint-derived dichlorodiphenyltrichloroethanes (DDTs) to a typical mariculture zone (South China): potential impact on aquafarming environment. Environ. Pollut. 159, 3700–3705.

Zeng, E.Y., Tsukada, D., Diehl, D.W., 2004. Development of solid-phase microextraction-based method for sampling of persistent chlorinated hydrocarbons in an urbanized coastal environment. Environ. Sci. Technol. 38, 5737–5743.